Journal of Hazardous Materials 164 (2009) 502–509

Contents lists available at ScienceDirect

Journal of Hazardous Materials

journal homepage: www.elsevier.com/locate/jhazmat

Removal of tartrazine from aqueous solutions by strongly basic polystyrene anion exchange resins

Monika Wawrzkiewicz*, Zbigniew Hubicki

Maria Curie – Sklodowska University, Faculty of Chemistry, Department of Inorganic Chemistry, 20-031 Lublin, M. Sklodowska Sq. 2, Poland

ARTICLE INFO

Article history:
Received 11 June 2008
Received in revised form 22 July 2008
Accepted 8 August 2008
Available online 15 August 2008

Keywords:
Dye
Removal
Sorption
Kinetics
Anion exchanger

ABSTRACT

The removal of tartrazine from aqueous solutions onto the strongly basic polystyrene anion exchangers of type 1 (Amberlite IRA-900) and type 2 (Amberlite IRA-910) was investigated. The experimental data obtained at 100, 200, 300 and 500 mg/dm^3 initial concentrations at 20 °C were applied to the pseudo-first order, pseudo-second order and Weber–Morris kinetic models. The calculated sorption capacities ($q_{e,cal}$) and the rate constant of the first order adsorption (k_1) were determined. The pseudo-second order kinetic constants (k_2) and capacities were calculated from the plots of t/q_t vs. t, $1/q_t$ vs. $1/t$, $1/t$ vs. $1/q_t$ and q_t/t vs. q_t for type 1, type 2, type 3 and type 4 of the pseudo-second order expression, respectively. The influence of phase contact time, solution pH and temperature on tartrazine removal was also discussed. The FTIR spectra of pure anion exchangers and those loaded with tartrazine were recorded, too.

1. Introduction

Dyes represent a very important group of water pollutants which appear in the effluents discharged from textile, leather, food processing, paper and dye manufacturing industries [1–5]. Today there are more than 10,000 dyes commercially available and the estimates indicate that about 10–15 % of synthetic dyes used are lost in waste streams during the processing operations [1,5–8]. Strongly coloured effluents not only create environmental and aesthetic problems, but can also affect the aquatic life and food web as most of them are mutagenic and carcinogenic [5]. The conventional methods of colour removal from industrial effluents involve many techniques, such as biological treatments [9–11], membrane technology [12], coagulation [13,14] and oxidation [5,15]. At present, the most common treatment method for effective dyestuff removal is adsorption [3,6,8]. Adsorption is found to be superior to other techniques in terms of initial costs, simplicity of design, ease of operation and insensitivity to toxic substances. Numerous studies are focused on utilization of wastes containing dyes using different sorbents. Almost all the papers related to adsorption techniques for colour removal from industrial effluents are based on studies employing activated carbon [7]. The high costs of activated carbon sometimes make its use limited. So many researchers have tried to search for alternative materials, which are relatively inexpensive and at the same time characterized reasonably adsorptive efficiency. Of many examples reported in literature, the following may be mentioned: rice [1] and peanut hull [16], sugarcane dust [17], pine sawdust [18], kohlrabi peel [8], orange peel [19], red mud and fly ash [6,20], chitosan and chitin [21], etc. There is still very little information in literature about removal of dyes using ion-exchangers [22,23]. Only Karcher et al. [23] proved that weakly and strongly basic anion exchange resins of commercial names Lewatit S6328A and Lewatit MP-62 exhibit good sorption characteristics for reactive dyes (Reactive Red 120, Reactive Red 198, Reactive Black 5) contained in wastewaters from textile industry. Complete regeneration without loss of capacity can be carried out using NaOH solutions or alkaline methanol–water mixtures [22,23]. These results suggest that anion exchangers in general could be effective sorbents for dyes removal.

The aim of this study was, therefore, to screen and apply commercially available macroporous polystyrene anion exchangers: Amberlite IRA-900 and IRA-910 for tartrazine removal from aqueous solutions. The effects of initial dye concentrations, phase contact time, solution pH as well as temperature on tartrazine adsorption were investigated. The experimental data were analyzed using the pseudo-first and second order kinetic models as well as the intraparticle diffusion equation. Kinetic constants were calculated.

Tartrazine is the best known and one of the most commonly used food additives. It is found in the following food stuffs: soft drinks, instant puddings, flavored chips, custard powder, soups, sauces, ice cream, candy, chewing gum, marzipan, jam, jelly,

* Corresponding author. Tel.: +48 81 537 57 38; fax: +48 81 533 33 48.
E-mail address: m.wawrzkiewicz@op.pl (M. Wawrzkiewicz).

0304-3894/$ – see front matter © 2008 Elsevier B.V. All rights reserved.
doi:10.1016/j.jhazmat.2008.08.021

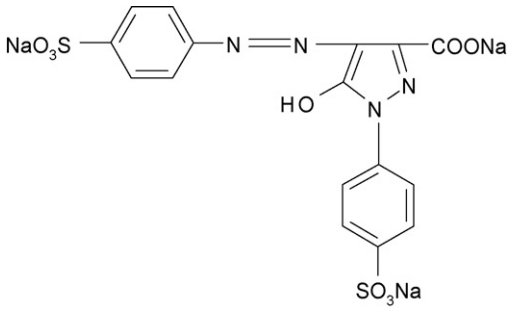

Fig. 1. Chemical structure of tartrazine, $C_{16}H_9N_4Na_3O_9S_2$.

marmalade, mustard, yogurt and many convenience foods including glycerin, lemon and honey products. Soaps, hair products, moisturizers, crayons, stamp dyes, vitamins, antacids, medicinal capsules also can contain tartrazine. Tartrazine appears to cause the most allergic and/or intolerance reactions of all the azo dyes, particularly amongst those with an aspirin intolerance and asthmatics. Tartrazine sensitivity is mainly manifested by urticaria. Other reactions can include migraine, blurred vision, itching [24–27].

2. Experimental

2.1. Materials

The molecular structure of 4,5-dihydro-5-oxo-1-(4-sulfophenyl)-4-[(4-sulfophenyl)azo]-1H-pyrazole-3-carboxylic acid trisodium salt (Sigma Aldrich, Germany) known as tartrazine (E102, Acid Yellow 23, FD&C Yellow 5, C.I. Food Yellow 4) is shown in Fig. 1.

Tartrazine solutions were prepared by dissolving the accurately weighed amount of dye in 1 dm^3 of distilled water.

In order to obtain the tartrazine solution of different initial pH, small amounts of 1 M HCl or 1 M NaOH (POCh, Poland) were added.

The properties of applied anion exchange resins are presented in Table 1.

2.2. Batch studies

The adsorption of tartrazine onto Amberlite IRA-900 and IRA-910 was studied by means of laboratory batch method. The samples of dry resin (0.25 g) were shaken mechanically (thermostatic shaker; Elphin +358S, Poland) with 25 cm^3 of corresponding dye solution for 1–240 min at 20–50 °C. The agitation speed was 170 rpm. Dye solutions of four different initial concentrations (100, 200, 300 and 500 mg/dm^3) were used.

At the end of the predetermined time interval, the anion exchanger was removed by the filtration and the dye concentration was determined using the UV-VIS spectrophotometer (specord M42; Carl Zeiss Jena, Germany) at the maximum absorbance wavelength (430 nm).

The data obtained from the sorption experiments were used to calculate the adsorption capacity, q_t (mg/g) from Eq. (1):

$$q_t = \frac{(C_0 - C_t)}{w} \times V \quad (1)$$

where C_0 and C_t are the concentrations of the dye in the solution before and after sorption respectively (mg/dm^3), V is the volume of the solution (dm^3) and w is the mass of the dry anion exchanger (g).

From these experiments the effect of phase contact time, initial dye concentration, pH and temperature was investigated.

All collected values in this paper are the average of three independent experiments.

Kinetic experiments related to the effect of initial concentrations were performed at the natural pHs (pH 4.55) of solutions (pH-meter; CX-742 Elmetron, Poland).

The differences in the spectra of anion exchangers before and after sorption of tartrazine were investigated by using the FTIR technique (spectrometer; type 1725X, Perkin-Elmer, Germany).

2.3. Determination of the distribution coefficients and resin capacities

The dynamic procedures were applied. The one-centimetre diameter columns were filled with swollen anion exchangers in the amount of 10 cm^3. Then tartrazine solution of the initial concentration 100 mg/dm^3 was passed through the anion exchanger bed at the rate of 0.8 cm^3/cm^2 min. The eluate was collected in the fractions and the tartrazine content was determined.

The mass (K_d) and bed (K'_d) distribution coefficients of tartrazine as well as working ion exchange capacities (C_r) were calculated from the breakthrough curves according to the Eqs. (2) and (3):

$$K_d = \frac{U - U_0 - V}{m_j} \quad (2)$$

where U is the effluent volume at $C = C_0/2$ (dm^3), U_0 is the dead volume in the column (liquid volume in the column between the bottom edge of ion-exchanger bed and the outlet) (dm^3), V is the void (inter-particle) ion exchanger bed volume (which amounts to ca. 0.4 of the bed volume) (dm^3), m_j is the dry ion exchanger mass (g).

$$K'_d = K_d d_z \quad (3)$$

where d_z is the bed density (g/dm^3) [28].

Working (C_w) ion exchange capacities are expressed in mg of tartrazine per cm^3 of swollen anion exchanger. The amount of the dye loaded on the anion exchanger was calculated by mass balance.

Table 1
Anion exchangers characteristic

Properties	Amberlite IRA-900	Amberlite IRA-910
Functional groups	Strongly basic, type 1 $-N^+(CH_3)_3$	Strongly basic, type 2 $-N^+(CH_3)_2C_2H_4OH$
Matrix	Polystyrene, macroporous	
Physical form	Pale yellow beads	White beads
Ionic form as shipped	Chloride	Chloride
Total ion-exchange capacity (eq/dm^3)	≥1.0	≥1.0
Moisture holding capacity (%)	58–64	54–61
Harmonic mean size (mm)	0.65–0.82	0.53–0.80
Maximum operating temperature (°C)	60	60
Producer	Rohm & Haas Co., France	

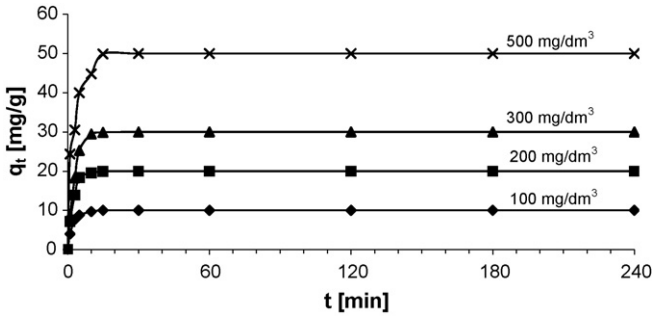

Fig. 2. Influence of phase contact time and initial concentration on tartrazine uptake at 20 °C by the strongly basic anion exchanger of type 1 Amberlite IRA-900.

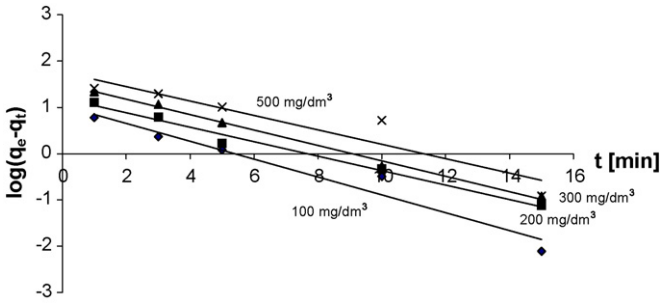

Fig. 3. Pseudo-first order model fit to the data describing the effect of initial tartrazine concentration on sorption kinetics using Amberlite IRA-900 at 20 °C.

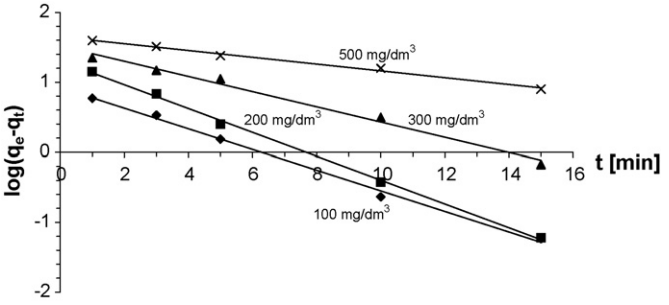

Fig. 4. Pseudo-first order model fit to the data describing the effect of initial tartrazine concentration on sorption kinetics using Amberlite IRA-910 at 20 °C.

3. Results and discussion

3.1. Effect of phase contact time and initial dye concentration

A series of contact time experiments for tartrazine has been carried out with the initial dye concentration from 100 to 500 mg/dm^3 at 20 °C. Fig. 2 shows that the amount of the adsorbed dye onto the strongly basic anion exchanger of $-N^+(CH_3)_3$ functional groups increased with time. The contact time necessary to reach equilibrium was 20 min. The sorption capacities q_t increase from 9.99 to 49.88 mg/g with the increase in initial concentration from 100 to 500 mg/dm^3.

The equilibrium uptake in the case of Amberlite IRA-910 occurred after 30 min. The sorption capacities using Amberlite IRA-910 were equal to 9.94, 19.93, 29.33 and 49.96 mg/g for the dye solutions of the initial concentrations 100, 200, 300 and 500 mg/dm^3, respectively.

The initial dye concentration had little influence on the time of contact necessary to reach equilibrium.

3.2. Kinetic parameters

The adsorption process proved to be effective for the removal of various pollutants from aqueous solutions. The prediction of batch kinetics is necessary for designing of sorption systems. Chemical kinetics explains the rate of chemical reactions. The nature of sorption process depends on physical or chemical characteristics of the adsorbent and also on the system conditions. Kinetic models based on the concentration of solute and on the dose of sorbent have been proposed by several researchers [29].

In order to investigate the mechanism of sorption, the rate constant of chemical sorption and intraparticle diffusion for the dyes were determined using the equations of the pseudo-first order system by Lagergren, pseudo-second order mechanism and intraparticle diffusion by Weber and Morris, respectively [29–33].

3.2.1. Lagergen pseudo-first order kinetics

The Langergren pseudo-first order rate expression is generally described using the following equation:

$$\frac{dq_t}{dt} = k_1(q_e - q_t) \quad (4)$$

where q_e and q_t are the amounts (mg/g) of dye adsorbed at equilibrium and at time t (min) respectively; and k_1 is the constant rate (1/min).

After integration by applying the boundary conditions ($q_t = 0$ at $t = 0$ and $q_t = q_t$ at $t = t$), Eq. (4) can be rearranged for the linearized data plotting:

$$\log(q_e - q_t) = \log(q_e) - \frac{k_1}{2.303}t \quad (5)$$

In order to confirm the applicability of the model, the plot of $\log(q_e - q_t)$ against t should be a straight line. In a real first-order process, experimental $\log(q_e)$ should be equal to the intercept of the straight line [30,34,35].

Figs. 3 and 4 show the $\log(q_e - q_t)$ vs. t plots taking into account the tartrazine initial concentration using Amberlite IRA-900 and IRA-910 in sorption experiments, respectively. The rate constants k_1 were calculated from the slopes of Figs. 3 and 4. It was noticed that the rate constants k_1 decreased with the increase in the initial dye concentration, some deviations were observed for the solution containing 200 mg/dm^3 of tartrazine. The correlation coefficients were high, ranging from 0.994 to 0.882 and from 0.996 to 989 for the anion exchangers of type 1 and type 2, respectively (Table 2). However, the calculated equilibrium capacities $q_{e,cal}$ according to the Langergren pseudo-first order rate expression are in good agreement with the values of experimental capacities $q_{e,exp}$ for solutions of the initial concentrations: 100, 200 and 300 mg/dm^3, the better results were obtained using the pseudo-second order equations.

Table 2
Pseudo-first order kinetic parameters for anion exchangers of type 1 and type 2

Parameters	Initial concentration			
	100 mg/dm^3	200 mg/dm^3	300 mg/dm^3	500 mg/dm^3
Amberlite IRA-900				
$q_{e,exp}$ (mg/g)	10.0	20.0	30.0	50.0
$q_{e,cal}$ (mg/g)	10.966	15.668	32.043	57.654
k_1 (1/min)	0.445	0.359	0.383	0.359
r^2	0.954	0.985	0.994	0.882
Amberlite IRA-910				
$q_{e,exp}$ (mg/g)	10.0	20.0	30.0	50.0
$q_{e,cal}$ (mg/g)	8.404	20.126	32.903	44.559
k_1 (1/min)	0.339	0.392	0.250	0.112
r^2	0.996	0.998	0.989	0.992

Table 3
Comparison of the pseudo-second order models

Type	Linear form	Plot
Type 1 pseudo-second	$\frac{t}{q_t} = \frac{1}{k_2 q_e^2} + \frac{1}{q_e} t$	t/q_t vs. t
Type 2 pseudo-second	$\frac{1}{q_t} = \left(\frac{1}{k_2 q_e^2}\right)\frac{1}{t} + \frac{1}{q_e}$	$1/q_t$ vs. $1/t$
Type 3 pseudo-second	$\frac{1}{t} = \frac{k_2 q_e^2}{q_t} - \frac{k_2 q_e^2}{q_e}$	$1/t$ vs. $1/q_t$
Type 4 pseudo-second	$\frac{q_t}{t} = k_2 q_e^2 - \frac{k_2 q_e^2 q_t}{q_e}$	q_t/t vs. q_t

3.2.2. Comparison of four types of pseudo-second order kinetic models

The pseudo-second order kinetic rate equation is expressed as:

$$\frac{dq_t}{dt} = k_2(q_e - q_t)^2 \quad (6)$$

where q_e and q_t are the amounts (mg/g) of dye adsorbed at equilibrium and at time t (min), respectively; and k_2 is the constant rate of the pseudo-second order adsorption (g/mg min).

After taking into account the boundary conditions, $q_t = 0$ at $t = 0$ and $q_t = q_t$ at $t = t$, the integrated form of Eq. (6) can be rearranged to obtain Eq. (7):

$$\frac{t}{q_t} = \frac{1}{k_2 q_e^2} + \frac{1}{q_e} t \quad (7)$$

and

$$h = k_2 q_e^2 \quad (8)$$

where h is the initial sorption rate (mg/g min).

The values of k_2 and q_e can be determined from the slope and intercept of the plot t/q_t vs. t, respectively. This dependence is defined as type 1 of the pseudo-second order expression.

Similarly, the pseudo second-order kinetic constant k_2 and q_e can be calculated from the plots of $1/q_t$ vs. $1/t$, $1/t$ vs. $1/q_t$ and q_t/t vs. q_t for type 2, type 3 and type 4 of the pseudo-second order expressions, respectively [31,32]. Table 3 shows the linear forms of Eq. (7) [36].

The calculated kinetic constants, according to the four linear forms of the pseudo-second order model at different food dye concentrations, are compared in Tables 4 and 5. Figs. 5–8 illustrate the experimental data using the equation of four pseudo-second kinetic models (types 1–4) for the sorption of tartrazine on Amberlite IRA-900 from the solution of initial concentration 100–500 mg/dm^3 at 20 °C. Similar patterns were obtained using Amberlite IRA-910. It was observed that k_2, h and $q_{e,cal}$ obtained from the four linear forms of the pseudo-second order equations were different.

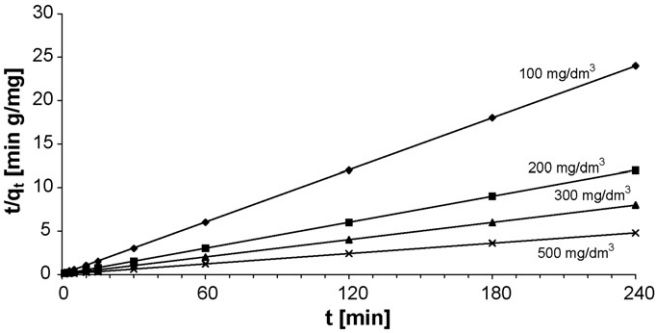

Fig. 5. The fitting of type 1 of the pseudo-second order model for tartrazine sorption on Amberlite IRA-900 for different initial concentrations at 20 °C.

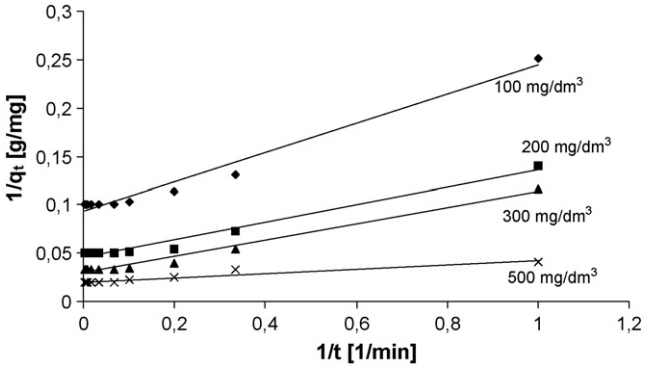

Fig. 6. The fitting of type 2 of the pseudo-second order model for tartrazine sorption on Amberlite IRA-900 for different initial concentrations at 20 °C.

Kinetics sorption of tartrazine from the solutions of the initial concentrations ranging from 100 to 500 mg/dm^3 on both strongly basic anion exchangers was well-described using model 1 of the pseudo-second expression. It was confirmed by the values of r^2 (0.999). The high values of r^2 confirm that the sorption process follows a pseudo-second order mechanism. The calculated sorption capacities were in very good agreement with the experimental

Table 4
Pseudo-second order kinetic parameters obtained from the linear forms at different initial concentration of tartrazine using Amberlite IRA-900 at 20 °C

Type	Parameters	Initial concentration of tartrazine			
		100 mg/dm^3	200 mg/dm^3	300 mg/dm^3	500 mg/dm^3
Types 1–4	$q_{e,exp}$ (mg/g)	10.0	20.0	30.0	50.0
Type 1	$q_{e,cal}$ (mg/g)	10.034	20.076	30.164	50.25
	k_2 (g/mg min)	0.175	0.077	0.036	0.022
	h (mg/g min)	17.635	31.259	32.733	56.631
	r^2	0.999	0.999	0.999	0.999
Type 2	$q_{e,cal}$ (mg/g)	10.741	21.857	33.761	49.659
	k_2 (g/mg min)	0.057	0.023	0.010	0.018
	h (mg/g min)	6.608	11.002	11.940	44.405
	r^2	0.976	0.975	0.980	0.929
Type 3	$q_{e,cal}$ (mg/g)	10.817	22.056	34.104	49.995
	k_2 (g/mg min)	0.055	0.022	0.010	0.016
	h (mg/g min)	6.449	10.725	11.705	41.274
	r^2	0.976	0.934	0.980	0.930
Type 4	$q_{e,cal}$ (mg/g)	11.722	7.967	37.844	24.310
	k_2 (g/mg min)	0.046	−0.218	0.004	−0.067
	h (mg/g min)	6.297	−13.853	6.374	−39.747
	r^2	0.957	0.668	0.974	0.863

Table 5
Pseudo-second order kinetic parameters obtained from the linear forms at different initial concentration of tartrazine using Amberlite IRA-910 at 20 °C

Type	Parameters	Initial concentration of tartrazine			
		100 mg/dm^3	200 mg/dm^3	300 mg/dm^3	500 mg/dm^3
Types 1-4	$q_{e,exp}$ (mg/g)	10.0	20.0	30.0	50.0
Type 1	$q_{e,cal}$ (mg/g)	10.041	20.096	30.299	51.013
	k_2 (g/mg min)	0.144	0.061	0.019	0.0006
	h (mg/g min)	14.528	24.752	17.758	14.412
	r^2	0.999	0.999	0.999	0.999
Type 2	$q_{e,cal}$ (mg/g)	10.477	22.673	32.254	49.071
	k_2 (g/mg min)	0.067	0.016	0.009	0.005
	h (mg/g min)	6.778	8.297	9.899	12.482
	r^2	0.988	0.972	0.995	0.977
Type 3	$q_{e,cal}$ (mg/g)	10.511	22.991	32.346	49.904
	k_2 (g/mg min)	0.061	0.015	0.009	0.005
	h (mg/g min)	6.699	8.067	9.850	12.189
	r^2	0.988	0.972	0.995	0.976
Type 4	$q_{e,cal}$ (mg/g)	11.299	6.994	32.743	11.489
	k_2 (g/mg min)	0.049	−0.236	0.006	−0.109
	h (mg/g min)	6.201	−11.539	5.957	−14.516
	r^2	0.972	0.709	0.864	0.945

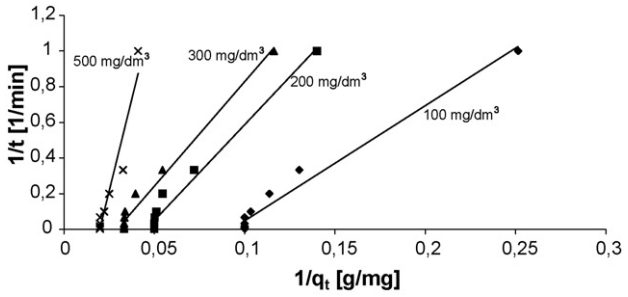

Fig. 7. The fitting of type 3 of the pseudo-second order model for tartrazine sorption on Amberlite IRA-900 for different initial concentrations at 20 °C.

sorption capacities (Tables 4 and 5). This also shows the applicability of type 1 of the pseudo-second order model in predicting the kinetics of tartrazine adsorption onto Amberlite IRA-900 and Amberlite IRA-910. It is generally assumed that a sorption process that fits the pseudo-second order kinetic model is the one controlled by chemisorption [11,35].

There was a good correlation of experimental capacities with those calculated $q_{e,cal}$ for tartrazine solutions using the linear forms of types 2 and 3 of the pseudo-second order kinetic expression. The values $q_{e,cal}$ were slightly higher than their experimental equivalents.

It was confirmed by the values of r^2 ranging from 0.929 to 0.995. There was observed the decrease in k_2 values with the increasing initial tartrazine concentration.

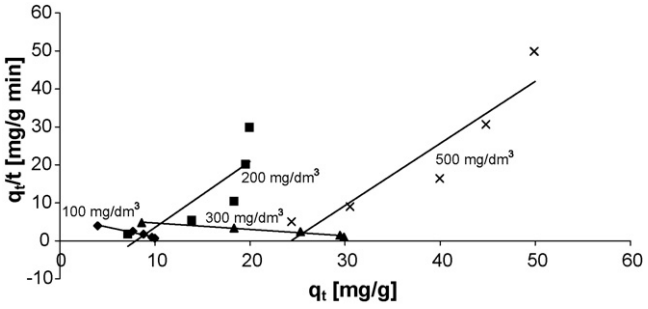

Fig. 8. The fitting of type 4 of the pseudo-second order model for tartrazine sorption on Amberlite IRA-900 for different initial concentrations at 20 °C.

Type 4 of the pseudo-second order expression represented very poorly the kinetic data of tartrazine. The lower r^2 values, from 0.668 to 0.974 for Amberlite IRA-900 and from 0.709 to 0.972 for Amberlite IRA-910, were obtained. Furthermore, for the initial dye concentrations 200 and 500 mg/dm^3, type 4 pseudo-second order expression produced negative k_2 and h values, which was experimentally and practically impossible.

3.2.3. Weber and Morris intraparticle diffusion model

Weber and Morris in 1963 [11,35] made the assumption that sorption is proportional to the square root of contact time:

$$q_t = k_i t^{0.5} \quad (9)$$

where k_i is the intraparticle diffusion rate (mg/g min$^{0.5}$).

The intraparticle diffusion model controls the sorption when the graph of q_t against $t^{0.5}$ is a straight line passing through the origin [11,37].

Fig. 9 illustrates the intraparticle diffusion kinetics of tartrazine at various initial concentrations at 20 °C on Amberlite IRA-900. The values of intraparticle diffusion rates k_i calculated from the slope of the plots q_t vs. $t^{0.5}$ increased from 0.210 to 1.227 mg/g min$^{1/2}$ and from 0.233 to 2.289 mg/g min$^{1/2}$ with the increase in the initial concentrations from 100 to 500 mg/dm^3 for Amberlite IRA-900 and Amberlite IRA-910, respectively. The values of r^2 are very low (<0.453 for Amberlite IRA-900 and <0.606 for Amberlite IRA-910). As shown in Fig. 9, with initial dye concentration increase, some deviations from intraparticle diffusion kinetics are observed. This can be attributed to some repulsion

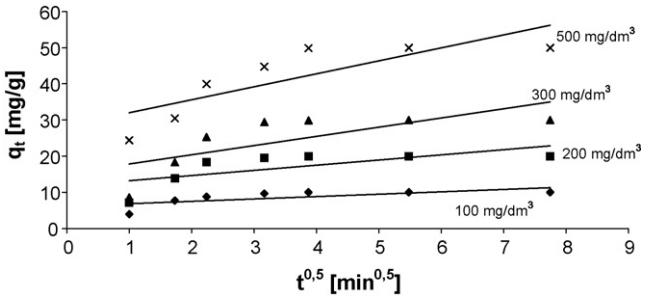

Fig. 9. Effect of initial dye concentration on the intraparticle diffusion kinetics of tartrazine on Amberlite IRA-900 at 20 °C.

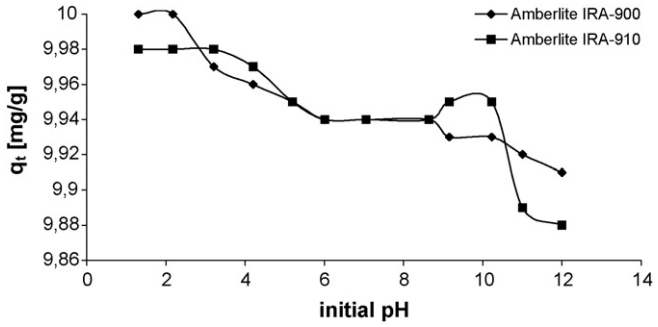

Fig. 10. Effect of initial pH on tartrazine removal from solution of initial concentration 100 mg/dm^3 using the strongly basic anion exchangers of types 1 and 2 (t = 45 min).

between adsorbent and adsorbate molecules due to concentration density.

3.3. Effect of pH

Solution pH is an important factor controlling the surface charge of the adsorbent and the degree of ionization of the adsorbate in the solution [38]. Fig. 10 shows the relationship between initial pH of tartrazine solutions and the adsorption capacity using the anion exchange resins of type 1 (Amberlite IRA-900) and type 2 (Amberlite IRA-910). Decrease in sorption capacity with the increasing initial concentration was observed. The system pH changed from 1.5 to 6.9 and from 1.2 to 10.7 during tartrazine adsorption at the initial solution pH of 1.3–12 by Amberlite IRA-900 and IRA-910, respectively.

In aqueous solution, tartrazine ($R'(SO_3)_2Na_2$) was dissolved and the strongly acidic sulfonate groups of the dye were dissociated and converted to anionic dye ions:

$$R'(SO_3)_2Na_2 \xrightarrow{H_2O} R'(SO_3)_2{}^{2-} + 2Na^+$$

The adsorption process then proceeded due to the interaction between the anionic dye ($R'(SO_3)_2{}^{2-}$) and the functional groups of the anion exchanger in chloride form (RCl):

$$2RCl + R'(SO_3)_2{}^{2-} \rightarrow R_2(SO_3)_2R' + 2Cl^-$$

As follows from the above, tartrazine forms a stable ion pair in the anion exchanger phase, but the surface interactions with the aromatic ring must be also taken into account. Tartrazine contains groups (—OH, —COONa, —SO_3Na, —N=N—) that can participate in covalent, coulombic, hydrogen bonding or weak van der Waals forces. The occurrence of double bond serves to enhance the interaction between the dye and the anion exchanger macromolecule. The physical adsorption and π–π dispersion forces can arise from the aromatic nature of the resin and tartrazine [39].

3.4. Effect of temperature

The temperature dependence of tartrazine sorption onto strongly basic anion exchangers was studied with the constant initial concentration of 100 mg/dm^3. Fig. 11 shows the effect of temperature on the sorption of tartrazine by Amberlite IRA-910 as a function of contact time. The equilibrium sorption capacity slightly increased when the temperature of dye solution increased from 20 to 50 °C. The same effect of temperature was observed for the anion exchanger of type 1.

The fact that the sorption of tartrazine is in favour of temperature indicates that the mobility of the dye molecule increases with the temperature rise [40].

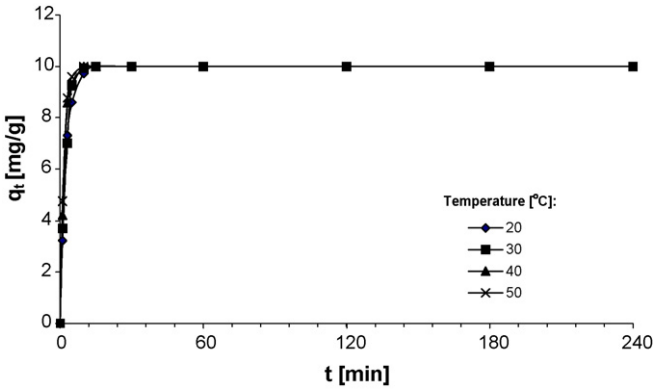

Fig. 11. Effect of temperature on tartrazine removal from solution of initial concentration 100 mg/dm^3 using the strongly basic anion exchanger of type 2 (t = 45 min).

3.5. Column experiments

The weight (K_d) and bed (K'_d) distribution coefficients as well as working (C_w) ion exchange capacities were calculated from the breakthrough curves. The breakthrough curves for tartrazine using Amberlite IRA-900 and IRA-910 are presented in Fig. 12.

K_d and K'_d are equal to 8.5 and 2.1 for the strongly basic anion exchanger of type 1. The values under discussion are higher for the anion exchanger of —$N^+(CH_3)_2C_2H_4OH$ functional groups (K_d = 11.6, K'_d = 2.2).

From the values of C_w (134.5 mg/cm^3 for Amberlite IRA-900 and 117.7 mg/cm^3 for Amberlite IRA-910) in the 100 mg/dm^3 tartrazine system, the studied anion exchangers can be presented in the following series:

Amberlite IRA-900 > Amberlite IRA-910

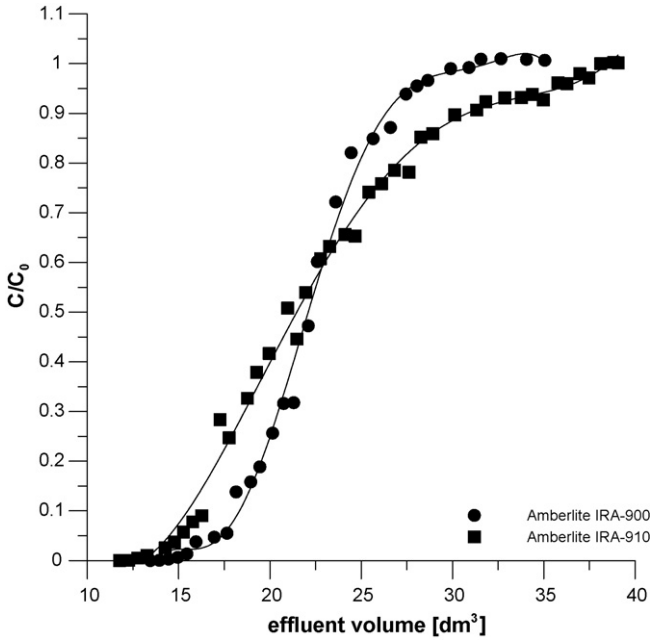

Fig. 12. Breakthrough curves of tartrazine determined for Amberlite IRA-900 and Amberlite IRA-910 (C_0 = 100 mg/dm^3, 10 cm^3 of swollen anion exchanger, volume velocity 0.8 cm^3/cm^2 min).

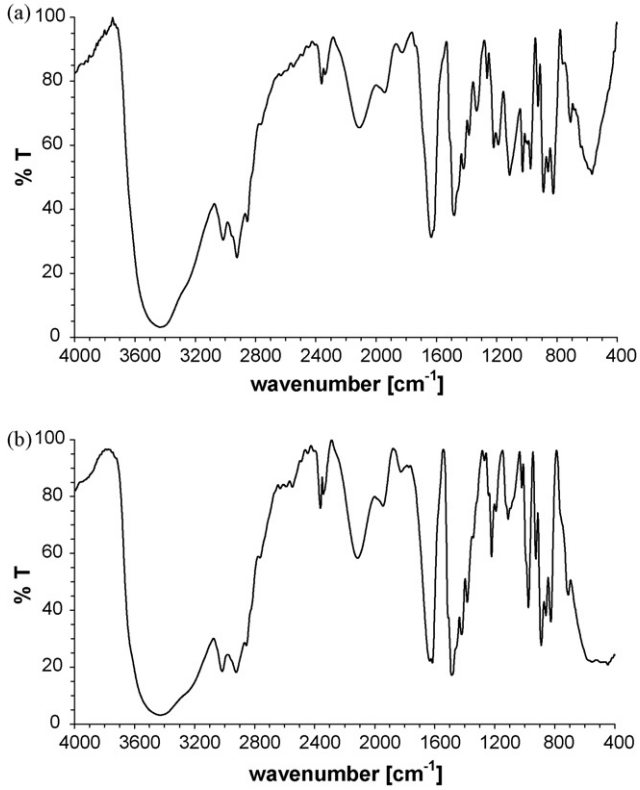

Fig. 13. a–b. FTIR spectra of Amberlite IRA-900 before (a) and after (b) sorption of tartrazine.

as far as their application is concerned in the removal of this dye from wastewaters.

3.6. FTIR analysis

The Fourier transform infrared spectroscopy method was used in the investigations of removal process of tartrazine using the strongly basic anion exchangers. The spectra of the anion exchangers were measured within the range of 400–4000 cm^{-1}.

The model spectra for Amberlite IRA-900 and Amberlite IRA-910 before and after loading with tartrazine are presented in Figs. 13a,b and 14a,b. The peaks around 3442 cm^{-1} for strong bands of the —OH stretching vibrations were observed for both anion exchangers. On the lower frequency side of this band some peaks at about 3018 cm^{-1}, 2922 cm^{-1}, related to the stretching vibrations of the ring C—H bonds and —CH_2 groups of the matrix (cross-linked polystyrene) of anion exchangers were observed (3018 cm^{-1} ν_{as}(C—H), 2922 cm^{-1} ν_{as} (—CH_2)). At 1630 cm^{-1} (δ(O—H)) the presence of water in the anion exchanger phase was found. The ring carbon–carbon stretching and the scissoring vibrations of the methylene groups (δ_{as}—CH_2) appeared at 1487and 1421 cm^{-1} as well as 1383 cm^{-1}. The deformation vibrations of 1,4-disubstituted benzene ring (S-DVB) were also noticed at 980 and 821 cm^{-1} [41–43]. The FTIR spectra of the strongly basic anion exchangers: Amberlite IRA-900 and IRA-910 before (Fig. 13a and 14a) and after (Fig. 13b and 14b) sorption of tartrazine are very similar. After the sorption the intensity of some bands changed. It was stated that in the spectra of the loaded anion exchangers (Figs. 13b and 14b) symmetric and asymmetric vibrations of —SO_3^- groups appeared at 1088 and 1149 cm^{-1}, respectively. At 1018 cm^{-1} asymmetric vibration of —S═O group was observed, too. It seems that these groups participate in dye binding.

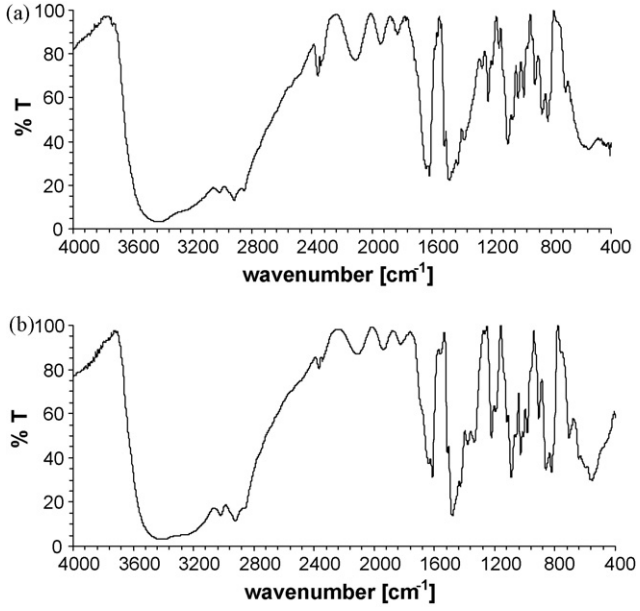

Fig. 14. a–b. FTIR spectra of Amberlite IRA-910 before (a) and after (b) sorption of tartrazine.

4. Conclusions

- The present study shows that the strongly basic polystyrene anion exchangers of type 1 (Amberlite IRA-900) and type 2 (Amberlite IRA-910) can be used as the adsorbent for the removal of tartrazine from its aqueous solutions.
- The amount of dye sorbed was found to vary with initial solution concentration, contact time and solution pH.

  The contact time necessary to reach equilibrium using Amberlite IRA-900 was 20 min., the sorption capacities q_e increase from 9.99 to 49.88 mg/g with the increase in tartrazine initial concentration from 100 to 500 mg/dm^3. The sorption capacities using Amberlite IRA-910 were equal to 9.94, 19.93, 29.33 and 49.96 mg/g for the dye solutions of the initial concentrations 100, 200, 300 and 500 mg/dm^3, respectively. The equilibrium was established after 30 min.

  The sorption capacities slightly decrease with initial solution pH increase for both anion exchangers.

  The equilibrium sorption capacity insignificantly increased when the temperature of dye solution increased from 20 to 50 °C using Amberlite IRA-900 and IRA-910.
- The sorption data were found to follow the pseudo-second order kinetic model of type 1. It was confirmed by the values of r^2 (0.999). There was a very good correlation of experimental capacities with those calculated $q_{e,cal}$ for tartrazine solutions, too. Type 4 of the pseudo-second order expression represented very poorly the kinetic data of tartrazine.
- The sorption mechanism of tartrazine on the strongly basic anion exchange resins: Amberlite IRA-900 and IRA-910 can be anion-exchanging. Interactions of the functional groups of tartrazine (—OH, —COONa, —SO_3Na, —N═N—) with the resin matrix could be result from covalent, coulombic and hydrogene bonding as well as weak van der Waals forces.
- Taking into account high values of the working ion exchange capacities Amberlite IRA-900 (134.5 mg/cm^3) and Amberlite IRA-910 (117.7 mg/cm^3) can find practical application in tartrazine removal from waste waters as well as prototypes of new chelating ion-exchangers for the transition metal ions sorption.

References

[1] D. Bilba, D. Suteu, T. Malutan, Removal of reactive dye brilliant red HE-3B from aqueous solutions by hydrolyzed polyacrylonitrile fibres: equilibrium and kinetics modelling, Cent. Eur. J. Chem. 6 (2008) 258–266.

[2] P.P. Selvam, S. Preethi, P. Basakaralingam, N. Thinakaran, A. Sivasamy, S. Sivanesan, Removal of rhodamine B from aqueous solution by adsorption onto sodium montmorillonite, J. Hazard. Mater. 155 (2008) 39–44.

[3] M. Wawrzkiewicz, Z. Hubicki, Use of weakly and strongly basic anion-exchange resins for the removal of indigo carmine from aqueous solutions, Przem. Chem. 87 (2008) 711–714 (in Polish).

[4] S.T. Ong, C.K. Lee, Z. Zainal, Removal of basic and reactive dyes using ethylenediamine modified rice hull, Biores. Technol. 98 (2007) 2792–2799.

[5] J.H. Sun, S.P. Sun, G.L. Wang, L.P. Qiao, Degradation of azo dye Amido black 10B in aqueous solutions by Fenton oxidation process, Dyes Pigments 74 (2007) 647–652.

[6] N. Dizge, C. Aydiner, E. Demirbas, M. Kobya, S. Kara, Adsorption of reactive dyes from aqueous solutions by fly ash: kinetic and equilibrium studies, J. Hazard. Mater. 150 (2008) 737–746.

[7] S. Aber, N. Daneshvar, S.M. Soroureddin, A. Chabok, K. Asadpour-Zeynali, Study of acid orange 7 removal from aqueous solutions by powdered activated carbon and modeling of experimental results by artificial neutral network, Desalination (2007) 87–95.

[8] R. Gong, X. Zhang, H. Liu, Y. Sun, B. Liu, Uptake of cationic dyes from aqueous solution by biosorption onto granular kohlrabi peel, Biores. Technol. 98 (2007) 1319–1323.

[9] T. Robinson, G. McMullan, R. Marchant, P. Nigam, Remediation of dyes in textile effluent: a critical review on current treatment technologies with a proposed alternative, Biores. Technol. 77 (2001) 247–255.

[10] M.H. Vijaykumar, P.A. Vaishampayan, Y.S. Shouche, T.B. Karegoudar, Decolourization of naphthalene-containing sulphonated azo dye by *Kerstersia* sp. VKY1, Enzyme Microb. Tech. 40 (2007) 204–211.

[11] C.L. Mack, B. Wilhelmi, J.R. Duncan, J.E. Burgess, A kinetic study of the recovery of platinum ions from an artificial aqueous solution by immobilized *Saccharomyces cerevisiae* biomass, Minerals Eng. 21 (2008) 31–37.

[12] T.H. Kim, C. Park, S. Kim, Water recycling from desalination and purification process of reactive dye manufacturing industry by combined membrane filtration, J. Cleaner Prod. 13 (2005) 779–786.

[13] B. Shi, G. Li, D. Wang, C. Feng, H. Tang, Removal of direct dyes by coagulation: the performance of preformed polymeric aluminum species, J. Hazard. Mater. 143 (2007) 567–574.

[14] J.W. Lee, S.P. Choi, R. Thiruvenkatachari, Evaluation of the performance of adsorption and coagulation processes for the maximum removal of reactive dyes, Dyes Pigments 69 (2006) 196–203.

[15] M. Muruganandham, M. Swaminathan, Decolourization of Reactive Orange 4 by Fenton and photo-Fenton oxidation technology, Dye Pigments 63 (2004) 315–321.

[16] R. Gong, Y. Sun, J. Chen, H. Liu, C. Yang, Effect of chemical modification on dye adsorption capacity of peanut hull, Dyes Pigments 67 (2005) 175–181.

[17] Y.S. Ho, W.T. Chiu, C.C. Wang, Regression analysis for the sorption isotherms of basic dyes on sugarcane dust, Biores. Technol. 96 (2005) 1285–1291.

[18] M. Özacar, İ.A. Şengil, A kinetic study of metal complex dye sorption onto pine sawdust, Process Biochem. 40 (2005) 565–572.

[19] M. Arami, N.Y. Limaee, N.M. Mahmoodi, N.S. Tabrizi, Removal of dyes from colored textile wastewater by orange peel adsorbent: equilibrium and kinetic studies, J. Colloid Interf. Sci. 288 (2005) 371–376.

[20] S. Wang, Y. Boyjoo, A. Chouebi, Z.H. Zhu, Removal of dyes from aqueous solution using fly as and red mud, Water Res. 39 (2005) 129–138.

[21] G. Annadurai, J.F. Lee, Equilibrium studies on the adsorption of acid dye into chitin, Environ. Chem. Lett. 6 (2008) 77–81.

[22] S. Karcher, A. Kornmüller, M. Jekel, Screening of commercial sorbents for the removal of reactive dyes, Dyes Pigments 51 (2001) 111–125.

[23] S. Karcher, A. Kornmüller, M. Jekel, Anion exchange resins for the removal of reactive dyes from textile wastewaters, Water Res. 36 (2002) 4717–4724.

[24] C. Collins-Williams, Clinical spectrum of adverse reactions to tartrazine, J. Asthma. 22 (1985) 139–143.

[25] J.R. Dipalma, Tartrazine sensitivity, Am. Fam. Physician 42 (1990) 1347–1350.

[26] R.E. Desmind, J.J. Trautlein, Tartrazine (FD&C Yellow 5) anaphylaxis: a case report, Ann. Allergy 46 (1981) 81–82.

[27] D.J. Baumgardner, Persistent urticaria caused by a common coloring agent, Postgrad. Med. 85 (1989) 265–266.

[28] J. Minczewski, J. Chwastowska, R. Dybczyński, Separation and Preconcentration Methods in Inorganic Trace Analysis, Wiley & Sons, Ltd., New York, 1982.

[29] K.V. Kumar, S. Sivanesan, Pseudo second order kinetic models for safranin onto rice husk: comparison of linear and non-linear regression analysis, Process Biochem. 41 (2006) 1198–1202.

[30] Y.S. Ho, G. McKay, Sorption of dyes from aqueous solution by peat, Chem. Eng. J. 70 (1998) 115–124.

[31] K.V. Kumar, Linear and non-linear regression analysis for the sorption kinetics of methylene blue onto activated carbon, J. Hazard. Mater. 137B (2006) 1538–1544.

[32] Y.S. Ho, Second-order kinetic model for the sorption of cadmium onto tree fern: a comparison of linear and non-linear methods, Water Res. 40 (2006) 119–125.

[33] M. Chabani, A. Amrane, A. Bensmaili, Kinetics of nitrates adsorption on Amberlite IRA-400 resin, Desalination 197 (2006) 117–124.

[34] Y.S. Ho, Removal of copper ions from aqueous solution by tree fern, Water Res. 37 (2003) 2323–2330.

[35] V. Vadivelan, K.V. Kumar, Equilibrium, kinetics, mechanism and process design for the sorption of methylene blue onto rice husk, J. Colloid Interf. Sci. 286 (2005) 90–100.

[36] K.V. Kumar, S. Sivanesan, Selection of optimum sorption kinetics: comparison of linear and non-linear method, J. Hazard. Mater. 134B (2006) 277–279.

[37] S.V. Mohan, S.V. Ramanaiah, B. Rajkumar, P.N. Sarma, Removal of fluoride from aqueous phase by biosorption onto algal biosorbent *Spirogyra* sp.-*IO2*: sorption mechanism elucidation, J. Hazard. Mater. 141 (2007) 465–474.

[38] N. Sakkayawong, P. Thiravetyan, W. Nakbanpote, Adsorption mechanism of synthetic reactive dye wastewater by chitosan, J. Colloid Interf. Sci. 286 (2005) 36–42.

[39] P. Pengthamkeerati, T. Satapanajaru, O. Singchan, Sorption of reactive dye from aqueous solution on biomass fly ash, J. Hazard. Mater. 153 (2008) 1149–1156.

[40] B. Acemioğlu, Batch kinetic study of sorption of methylene blue by perlite, Chem. Eng. J. 106 (2005) 73–81.

[41] D. Kołodyńska, J. Ryczkowski, Z. Hubicki, FT-IR/PAS studies of chelates adsorption on anion exchangers, Eur. Phys. J. Special Topics 154 (2008) 339–343.

[42] G. Socrates, Infrared and Raman Characteristic Group Frequencies: Tables and Charts, John Wiley & Sons, Ltd., Chichester, 2001.

[43] G. Wronski, S. Pasieczna-Patkowska, Z. Hubicki, Mechanism of sorption sulphoderivative organic chelating agents on strong base anion exchanger Amberlite IRA-402 by FT-IR/PAS and DRS methods, Eur. Phys. J. Special Topics 154 (2008) 377–380.